Structure-based prediction of free energy changes of binding of PTP1B inhibitors

Jing Wang*, Shek Ling Chan & Kal Ramnarayan
Structural Bioinformatics Inc., 10929 Technology Place, San Diego, CA 92127, U.S.A.

Summary

The goals were (1) to understand the driving forces in the binding of small molecule inhibitors to the active site of PTP1B and (2) to develop a molecular mechanics-based empirical free energy function for compound potency prediction. A set of compounds with known activities was docked onto the active site. The related energy components and molecular surface areas were calculated. The bridging water molecules were identified and their contributions were considered. Linear relationships were explored between the above terms and the binding free energies of compounds derived based on experimental inhibition constants. We found that minimally three terms are required to give rise to a good correlation (0.86) with predictive power in five-group cross-validation test ($q^2 = 0.70$). The dominant terms are the electrostatic energy and non-electrostatic energy stemming from the intra- and intermolecular interactions of solutes and from those of bridging water molecules in complexes.

Introduction

We describe, in the present paper, our recent studies on developing a binding free energy function and related procedures for prediction of activities and binding modes of the small molecule inhibitors toward an important therapeutic target, protein tyrosine phosphatase 1B (PTP1B).

Design of small molecule compounds inhibiting the enzymatic function of PTP1B is of great medicinal interest. It is actively being pursued in many academic [1] and industrial [2] organizations. It is appreciated that PTP1B is a negative regulator of insulin receptor signaling and a suitable drug target for treatment of insulin resistance associated with diabetes and obesity [3–7]. Clinical studies have found a correlation between insulin resistance states and levels of PTP1B expression in muscle and adipose tissues [8–10]. Recent PTP1B knockout studies revealed that mice lacking functional PTP1B exhibit increased

sensitivity toward insulin and are resistant to obesity [11].

PTP1B is a prototypical intracellular protein tyrosine phosphatase found in a wide variety of human tissues [12]. The exact roles of PTP1B in relation to insulin resistance are not fully understood. It has been demonstrated that the interaction of insulin with its receptor leads to the phosphorylation of certain tyrosine residues (1158, 1162 and 1163) within the receptor protein, thus activating the receptor kinase [13]. PTP1B, probably together with other phosphatases (LAR, PTPα and SH-PTP2) [14], dephosphorylate the activated insulin receptor. Recent studies with LAR knocked out mice have not shown altered glucose homeostasis, however [15]. The dephosphorylated insulin receptor loses the tyrosine kinase activity that is required for further down-stream signaling [13, 16].

Inhibition of PTP1B prevents, at least to some extent, the activated insulin receptor from being inactivated. In addition to the above function, PTP1B dephosphorylates a number of other receptor tyrosine kinases, including the EGF receptor and the PDGF receptor [17]. Development of specific inhibitors to PTP1B provides not only potential anti-diabetic drugs

*To whom correspondence should be addressed. E-mail: jing@strubix.com

but also chemical probes for clarification of the roles of PTP1B in normal cellular processes as well as in pathogenic pathways.

The three-dimensional structures of PTP1B in complex with various substrates and small molecule inhibitors have been solved by X-ray crystallography [18–20], making PTP1B a suitable target for structure-based drug design. However, most inhibitors reported so far are not qualified for *in vivo* testing, though one type of compounds has shown some activity in lowering the blood glucose levels in mice [21]. The existing compounds commonly suffer from having low potency and from bearing negatively charged groups that cause poor membrane permeability. Development of potent drug-like compounds is highly desired.

Prediction of binding potency of small molecule ligands is a critical step in rational drug design. There are traditionally two distinct approaches to address this problem. One is known as the quantitative structure-activity relationship (QSAR) study [22], in which a mathematical relationship between the calculable descriptors and experimental binding activities is derived for a set of existing compounds. The obtained relationship is applied to predict the activities of new compounds. This approach does not use the structural information about ligand-receptor complexes. The other approach is the calculation of binding free energy by performing molecular dynamics simulation or Boltzmann sampling on the corresponding free and bound state molecules. The typical methods of this approach are the free energy perturbation (see, for example, reference 23), harmonic well approximation [24] and exhaustive sampling [25]. Each of these approaches has serious limitations. The QSAR approach cannot give the details about ligand-receptor interactions that are important for drug design. Often, reasonable correlation can only be found for a selected subset of compounds sharing common scaffolds. Thus, the goal for predicting activities of novel compounds could not be reached. The simulation-based approach is only able to address the relative free energy changes stemming from minor modifications of compounds. It is time-consuming to the extent of seriously limiting its use.

The continuum electrostatic solvation model, supplemented with a cavity term, is considered promising for predicting free energy changes. Hou et al. [26] have recently used this approach to discriminate binding conformers in the complexes of EGF-R kinase and small molecule inhibitors. However, it has not been generally accepted that the approach could predict binding free energies without parameterization with a training set.

A novel approach for potency prediction has recently been explored in several laboratories [27–31], that involves deriving quantitative relationships between the binding free energies of compounds and the related molecular interaction energy components within and between compounds and protein targets. It typically proceeds from docking a set of existing compounds to a receptor, calculating various energy components and related properties, and correlating them with observed activities. Assuming a reliable correlation is found, the same protocols and parameters may be used for prediction of new compounds. Such a structure-based QSAR involves the details of molecular interaction. The free energy changes of binding are calculated with the input of certain system-dependent parameters. This approach allows one to gain an understanding of the driving forces in the related binding processes. The applicability on prediction of novel compounds is expected to be more general relative to the traditional QSAR approach, owing to the fact that the calculations are primarily based on First Principles. The success depends on the generality and accuracy of the force-field used, and on the formulation and approximation of the free energy functions. Our approach belongs to this category.

The structure-based QSAR approach has successfully been applied to the inhibitors of human immunodeficiency virus protease [27–29], estrogen receptor ligands [30], and thrombin inhibitors [31]. Alternatively, researchers used docking to obtain aligned 'bio-active' conformations of compounds [31–33] in order to perform comparative molecular field analysis [34]. Recently, a number of works have been done using similar approaches [35–39].

This is the first time that a structure-based QSAR approach is used for PTP1B inhibitors. Murthy and Kulkarin [40] have recently performed docking and molecular dynamics simulation with 16 PTP1B inhibitors, without seeking for quantitative correlation with experimental binding free energies. We docked 35 published compounds [2, 20, 41–45] based on the X-ray structures [18–20] of the complexes of the related compounds. We used a previously established equation [24, 46] in which the free energy change of a molecular process is regularly decomposed into solute enthalpy, solute solvation free energy, and solute configurational entropy terms. The first component is evaluated using force-field energies. The second component is approximated using molecular surface areas.

The third component is approximated using the number of rotatable bonds that are 'frozen' upon binding. We finally derived a binding free energy function which is a linear combination of six terms, including total electrostatic energy, total non-electrostatic energy, polar and nonpolar surface areas, number of rotatable bonds and number of bridging water molecules. These terms were evaluated for each of the compounds. Linear least-square fitting experiments were performed with the six terms to the experimental binding free energies, as well as with subsets of the terms in order to minimize the number of variables in fitting. We finally obtained a free energy function composed of three terms with a correlation coefficient of 0.86 to the experimental values. It was validated using the leave-one-out (LOO) cross-validation method ($q^2 = 0.67$). We further examined the predictability by dividing the compound set into five groups, and predicting each from the rest of the groups. A similar level of prediction ($q^2 = 0.70$) was obtained.

Another novelty of our method is the treatment of the contribution of bridging water. Our analysis of the results indicates that the bridging water molecules between ligand and protein significantly influence the complex structures. We developed a novel algorithm to add bridging water molecules to complex structures, and were able to predict most of the bridging water molecules observed in X-ray structures. We developed a method to calculate the energetic contributions of bridging water based on thermodynamic principles.

Methodology

Docking procedure

Seven crystal structures corresponding to the complexes of PTP1B with compounds 10, 11 and 19–23 (see Table 1 for PDB codes) were used as standard structures. The docking starting points for the other compounds were obtained by modifying these compounds in their X-ray structure positions. For example, compound 1 was obtained by removing the carboxylate of compound 10, and compound 4 was in turn obtained by changing the phosphate group of compound 1 into a tetrazolium ring. When added groups were related to the parent pieces by rotatable bonds, several starting conformations were generated to explore all the conformational possibilities. Each starting point, including X-ray structures, was energy-minimized using the Sybyl program [47] with

an MMFF94 force-field [48]. A distance dependent dielectric constant of 4r or 2r was used. The non-bonded cutoff distance was set to 14 Å. The Powell minimizer [49] was used. The convergence criterion of minimization was that the root-mean-square value of the energy gradients reached 0.01 kcal/mol/Å. The lowest energy minimum was taken as the docked structure for each compound. For each complex, the contributions to the total energy included the ligand atoms and any other atoms within 14 Å from any of the ligand atoms in the X-ray structure of 1BZJ (Table 1). The flexible part in energy minimization included the related ligand, any added water molecules, the side chains of all the residues in direct contact with the ligand in 1BZJ and residues 20, 21, 24, 29, 36, 47, 116, 120, 254, 258 and 263, and the full residues of 181 to 183.

Free energy function

Let us consider a process where a protein P, an inhibitor I and n water molecules W associate to form a complex P•I•nW:

$$P + I + nW \rightarrow P \bullet I \bullet nW$$
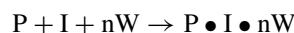
Let us consider the n bridging water molecules as 'solutes' and that all the solutes here are surrounded by implicit solvent medium. According to a mathematical demonstration [24, 46], the free energy change ΔG of the association is,

$$\Delta G = \Delta E + \Delta \Phi - T\Delta S_c \tag{1}$$

where ΔE corresponds to the change in the ensemble average of the solute-solute molecular energy including the contributions of the n waters, $\Delta \Phi$ corresponds to the change of solvation free energy of the solutes in the surrounding medium, ΔS_c corresponds to the change of entropy of the solutes, and T is the absolute temperature.

In the current studies, we do not intend to perform the time-consuming ensemble average calculation. We use instead the quantities calculated based on a representative conformation of a state to approximately replace the corresponding averaged values of that state. The representative conformation of a bound state corresponds to the lowest energy conformation obtained upon searching the torsion angle space of the part of a ligand not given in crystal structures. The representative conformation of a free state ligand was defined as the minimized conformation upon extraction of the ligand from the complex. The free energy

498

Table 1. Structures, direct or estimated K_i values, normalized K_i values and experimental binding free energies of the training and test set compounds.
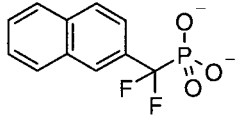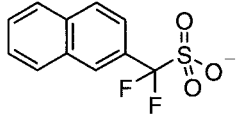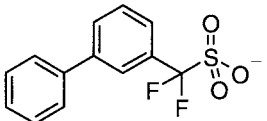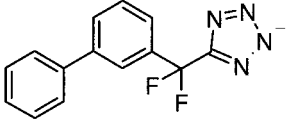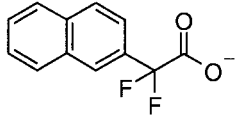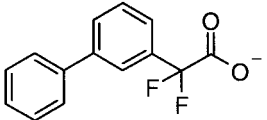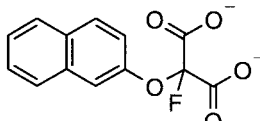
ID	structure	K_i (μM)	K_i [a] (μM)	ΔG^{ex} (kcal/mol)
1		15 [b] 28 [c] 58 [d] 179 [e-g, *]	45.7	2.278
2		75 [b]	228	3.237
3		49 [b, *]	149	2.983
4		98 [b]	298	3.396
5		98 [b, *]	298	3.396
6		273 [b]	831	4.007
7		185 [b]	563	3.775
8		136 [b]	414	3.592
9		107 [b]	326	3.449

Table 1. Continued.

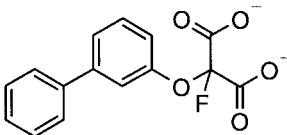| ID	structure	K_i (μM)	K_i [a] (μM)	ΔG^{ex} (kcal/mol)
10 [i]		22 [e, *]	5.7	1.034
11 [j]		12.4 [e, *]	3.17	0.687
12		25.0 [e, *]	6.4	1.104
13		2500 [e, *]	638	3.849
14		93 [f, *]	23.7	1.887
15		255 [f, *] 69 [d]	59.5	2.435
16		16 [d, *]	13.8	1.563

500

Table 1. Continued.

ID	structure	K_i (μM)	K_i a (μM)	ΔG^ex (kcal/mol)
17		16 d, *	13.8	1.563
18		73 d	63	2.47
19 k		68 g, *	17.4	1.701
20 l		200 g, *	51	2.344
21 m		1.4 g, *	0.36	-0.613
22 n		5.1 h, * 4.7 g, *	1.20	0.108

Table 1. Continued.
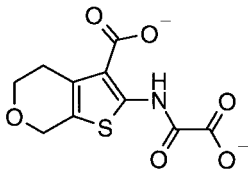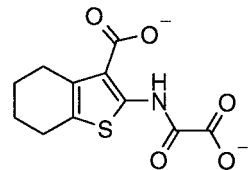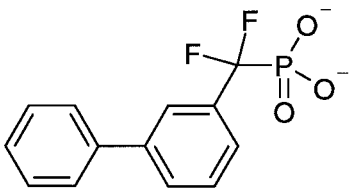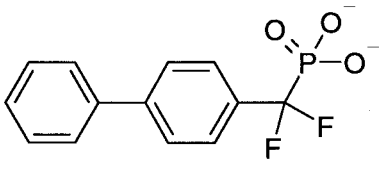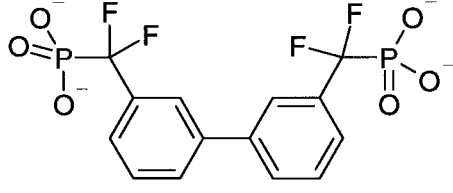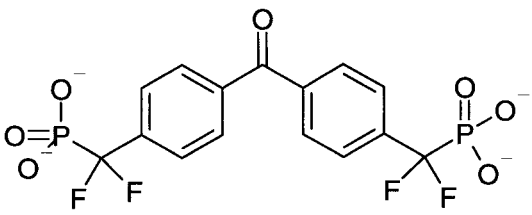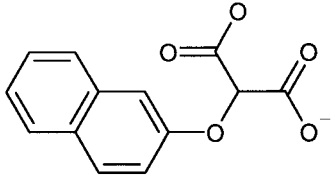
ID	structure	K_i (μM)	K_i [a] (μM)	ΔG^{ex} (kcal/mol)
23 [o,p]		63 [h,*]	14.8	1.607
24		39 [h,*]	9.2	1.321
25		10.5 [c] 6.4 [b]	18.3	1.732
26		63 [c]	103	2.761
27		13.5 [c]	22	1.841
28		3.0 [c]	4.9	0.947

Table 1. Continued.

ID	structure	K_i (µM)	K_i[a] (µM)	ΔG^{ex} (kcal/mol)
29		4.5 [c, *]	7.4	1.189
30		15 [c]	24	1.906
31		7.8 [c]	12.7	1.516
32		2.3 [c]	3.8	0.788
33		2.0 [c]	3.3	0.705
34		1.5 [c, *]	2.45	0.534

Table 1. Continued.

ID	structure	K_i (μM)	K_i [a] (μM)	ΔG^{ex} (kcal/mol)
35		2500 [g, *]	638	3.849

[a]Normalized K_i. [b–h]References 42–44, 41, 45, 2 and 20; [i–p]PDB entries 1BZJ, 1BZC, 1C84, 1C85, 1PTT, 1C88, 1C86, 1C87. *Direct measurement of K_i; the others in this column are estimated values based on $(IC_{50}/IC_{50}^*)K_i^*$ where the asterisk indicates the quantities of a compound with known K_i in the same reference.

difference derived from these representative conformations of bound and free states will primarily reflect loss of intermolecular interactions when a complex dissociates.

Equation 1 can be expanded as,

$$\Delta G = (E_{P\bullet I\bullet nW} - E_P - E_I - nE_W) + (\Phi_{P\bullet I\bullet nW} - \Phi_P - \Phi_I - n\Phi_W) + (-T\Delta S_P - T\Delta S_I) + (-TS_{nW} + nTS_W), \quad (2)$$

where $E_{P\bullet I\bullet nW}$, E_P, E_I and E_W, respectively, correspond to the energies of the complex and free state molecules; $\Phi_{P\bullet I\bullet nW}$, Φ_P, Φ_I, and Φ_W, respectively, correspond to the solvation free energies of the complex and free state molecules; ΔS_P and ΔS_I, respectively, correspond to the entropy changes of protein and inhibitor from free to bound states; and S_{nW} and S_W, respectively, correspond to the entropies of the n waters in complex and a single water in the free state.

Rearranging Eq. 2, one obtains,

$$\Delta G = (E_{P\bullet I\bullet nW} - E_P - E_I) + (\Phi_{P\bullet I\bullet nW} - \Phi_P - \Phi_I) + (-T\Delta S_P - T\Delta S_I) - n(E_W + \Phi_W - TS_W) - TS_{nw} \quad (3)$$

The terms in the last parentheses in Eq. 3 can be viewed as the free energy of a water molecule in the free state, which is constant.

The terms in the first parentheses can be evaluated based on force-field energies; those in the second parentheses are approximated by linear combination of the polar and nonpolar surface areas of the systems;

$-T\Delta S_P$ is neglected; $-T\Delta S_I$ is approximated with a linear function to the number m of rotatable bonds of inhibitor; and the last term, the entropy contribution of the n waters in complex, is approximated to be proportional to n. By separating the terms in the first parentheses into an electrostatic component and a non-electrostatic component, one can rewrite Eq. 3 as,

$$\Delta G = \Delta E^{ne} + \Delta E^e + \alpha \Delta A^{pol} + \beta \Delta A^{npol} + \gamma m + ng_w, \quad (4)$$

where ΔE^{ne} and ΔE^e, respectively, denote the changes in the total non-electrostatic energy and total electrostatic energy of the solutes (including the contributions of the n bridging water molecules); ΔA^{pol} and ΔA^{npol}, respectively, denote the changes in the polar surface area and nonpolar surface area; g_w is the opposite of the free energy of a water molecule in the free state plus the entropy contribution of a bridging water in the bound state; and α, β and γ are the coefficients relating the corresponding terms to the free energy contributions.

One notes that, in Eq. 4, the electrostatic term depends on the dielectric constant that is unknown for the studied environment, and the parameters α, β, γ and g_w are also undetermined. These parameters will be determined by least-square fitting of ΔG to experimental binding free energies.

Based on Eq. 4, the following linear function for the free energy change of binding can be established,

$$\Delta G = a_1 \Delta E^{ne} + a_2 \Delta E^e + a_3 \Delta A^{pol} + a_4 \Delta A^{npol} + a_5 m + a_6 n + C, \quad (5)$$

where parameters a_1 to a_6 and constant C are the coefficients to be determined by least-square fitting of ΔG to the experimental binding free energy ΔG^{ex}.

The experimental binding free energy is derived from the inhibition constant K_i of a compound as,

$$\Delta G^{ex} = kT \ln K_i, \qquad (6)$$

where k is Boltzmann's constant (kT = 0.596 kcal/mol at T = 300 K).

Calculation of energy components, surface areas and number of rotatable bonds

Each term in Eq. 5 was calculated for each compound using the docked complex and free state conformations of compound and protein. The free state conformation of a compound was obtained by extracting the compound from its complex and energy-minimizing it. A single free state conformation of protein was used, that was obtained by minimizing the X-ray structure of 1C85 without the ligand (choosing a different protein free state conformation will only change the constant term in fitting). All energy minimization was done with the same relevant conditions as for the docking process. The energy components were calculated using the same conditions. The surface areas were defined as the Connolly surface areas calculated using the Insight II program [50] with the default atom radii and 1.6 Å as water probe radius. The polar surface area was defined by the contributions from all the nitrogen, oxygen and fluorine atoms and the hydrogen atoms bonded to nitrogen and oxygen atoms. The non-polar surface area was defined by the contributions from all the tetrahedral carbon atoms and the hydrogen atoms bonded to them. All the other atoms were considered neutral and contribute to neither the polar nor the non-polar surface area. The number of rotatable bonds of a compound was obtained by counting the single bonds that are not involved in π-electron conjugation of the bracketing groups. Since rotation of a symmetrical group around a torsional angle is possible not only in free state but also in bound state, this degree of freedom will not contribute a large conformational entropy change in binding. The torsional angles relating to the rotation of symmetrical groups were therefore not counted in the m value of a compound.

Calculation of bridging water molecules

All of the initial bound water molecules were removed prior to docking of compounds. The lowest energy conformation of the complex of each compound was subject to the water addition calculation. Water molecules were first added to any location where a water molecule can form at least one hydrogen bond with protein and one with ligand and did not overlap with any solute atoms or other water atoms. The position of each water molecule was optimized to maximize the number of hydrogen bonds that could be formed in relation to the water molecule. In the cases that adjacent water molecules were interfering with each other, they were added in a way to maximize the number of hydrogen bonds formed in the locality, and to give rise to a unique pattern of water molecules. Then, the water molecules that were not qualified as 'bridging water' or were considered as part of 'bulk water' were removed. Specifically, any water molecules only bridging a pair of solute atoms hydrogen-bonded between themselves were removed. The degree of exposure of each added water molecule was calculated (Fig. 1). A regular icosahedron was centered on each water oxygen and a pseudo-atom was put at each vertex and the midpoint of each edge of an icosahedron, totaling 42 pseudo-atoms for each water molecule. A pseudo-atom has a radius of 1.5 Å and is always 2.5 Å away from the corresponding water oxygen. If a water molecule bears more than two pseudo-atoms that do not overlap with solute atoms, the water molecule is considered significantly exposed, or joining the bulk solvent, and is removed from the system. The complexes after adding bridging water molecules were minimized again.

Sources of K_i values

Precaution was taken to minimize the systematic errors of the K_i values reported in different papers. The K_i values used were based on seven references [2, 20, 41–45]. The K_i value of compound 1 was taken as the geometric mean (K_i^0) of the reported values of six sources. For the rest of the compounds reported from the same six references, the K_i values were normalized relative to compound 1 using $(K_i/K_i^1)K_i^0$, where K_i and K_i^1 are the values of a studied compound and compound 1 reported in a same reference, or $(IC_{50}/IC_{50}^1)K_i^0$ if only IC_{50} was available. If a compound is reported in more than one references, the geometric mean of the values derived from all the sources was taken. As for the compounds reported in the seventh reference (which does not contain compound 1), they were normalized via compound

22 which appears in the same reference and another reference containing compound 1.

Least-square fitting

The experimental binding free energy of each compound is derived from K_i using Eq. 6. The standard least-square fitting was performed to derive the parameters in Eq. 5 using these experimental binding free energies as the objective function together with the six terms calculated with the procedure described above. Fitting was also performed with some terms dropped in order to minimize the data noise (see Results section).

Quality of fit and cross-validation

The quality of fit after a fitting experiment is measured by r^2,

$$r^2 = 1 - \sum_i (\Delta G_i^{ex} - \Delta G_i)^2 / \sum_i (\Delta G_i^{ex} - \Delta G_M^{ex})^2, \tag{7}$$

where ΔG_i, ΔG_i^{ex} and ΔG_M^{ex} are respectively the predicted and experimental binding free energies of compound i and the arithmetic mean of the experimental binding free energies of all the compounds.

Leave-one-out cross-validation was performed by leaving out one compound at a time, and predicting the binding free energy of the compound with the parameters derived based on the rest of the compound set. After every compound has been predicted this way, the quality of prediction was measured using the q^2 value that is defined in a similar manner as in Eq. 7 except that ΔG_i is now predicted using a compound set lacking the compound to be predicted.

Cross-validation with five independent groups was performed by arbitrarily dividing the compound set into five groups with equal sizes. The binding free energies of the compounds of each group were predicted using the parameters derived based on the remaining four groups. Each group was predicted in turn. The quality of prediction was measured using q^2 with ΔG_i obtained under the current conditions.

Results

The compound set used for the present studies was collected from the previous publications. The criteria used in selecting compounds were as follows. (1)

If a reference reports the IC_{50} values for a set of compounds and the K_i values for at least one of the compounds, the compounds with available IC_{50} values in this reference are subject to further examination. And (2) if a reference does not contain a compound that is also reported in another reference so that the systematic errors of one reference relative to another can be estimated (see Methodology section), the reference will not be chosen. Using these criteria, we found 35 compounds from seven references. The identifications, chemical structures, direct or estimated K_i values, normalized K_i values and experimental binding free energies of these compounds are given in Table 1. It appears that the normalized K_i ranges from 0.36 to 831 μM spanning about 4.6 kcal/mol in free energy scale. All the compounds have at least one negative charge, probably due to the inherent requirement to occupy the phosphate-binding site in the catalytic site of PTP1B.

In order to assess the quality of docking structures, the seven complexes derived from X-ray crystallography are compared with the structures derived from docking. The compound identifications, PDB codes and the RMS deviations of ligand atoms between the docked structures and X-ray structures are given in Table 2. The RMS deviations were obtained by overlapping the protein α-carbon atoms of a docked complex with those of the corresponding X-ray structure. It appears that the docked structures are close to the X-ray structures with the RMS deviations fluctuating between 0.74 and 1.56 Å. The degree of deviations is expected given the resolutions of the X-ray structures. Visual inspection showed that the docked structures are generally close to the corresponding crystal structures with all the hydrogen bonds and hydrophobic contacts conserved. The relatively large RMS deviation for compound 21 is due to the displacement of the C-terminal atoms of the compound that make no interactions with PTP1B and are not well defined in the crystal structure.

The number of bridging water molecules visualized in X-ray structures, those predicted in our docking process and the deviations between the experimental and predicted positions of the corresponding bridging water molecules are given in the fourth through sixth columns in Table 2. In four crystal structures (1BZC, 1C84, 1C88 and 1C86), a bridging water molecule can be found in a location accepting hydrogen bonds from the backbone amide of Phe182 and the side chain amide of Gln266 and donating a hydrogen bond to a ligand atom (Figure 2). In two

Table 2. Comparison of docking results and crystal structures in terms of the dispositions of ligands and bridging water molecules.

Compound ID	PDB ID	Ligand RMS deviation[a]	Number of bridging waters in crystal	Predicted number of bridging waters	Bridging water RMS deviation[b]
10	1BZJ	0.91	1	2	0.51
11	1BZC	1.19	1	2	0.50
19	1C84	0.86	1	2	0.53
20	1C85	0.74	1	2	0.74
21	1PTT	1.56	0	2	–
22	1C88	0.86	1	2	0.54
23	1C86	0.81	1	2	0.63

[a]In Å.
[b]In Å. The deviations for the predicted waters that are vacant in crystal structures are set to zero.

other crystal structures (1BZJ and 1C85), a bound water molecule is found in a different location, forming hydrogen bonds with the side chains of Tyr46 and Asp181. However, these water molecules did not concomitantly appear in the same crystal structures, although voids exist to allow this to happen. One crystal structure (1PTT) did not show water molecules in the corresponding places with similar unoccupied space. Our program generated water molecules for both the places for all the structures. The positioning of water molecules with our program was quite accurate with deviations from crystal water positions less than 0.74 Å.

In Table 3 the changes in non-electrostatic energy, electrostatic energy, polar surface area and non-polar surface area in the binding of each compound, the number of rotatable bonds of each compound and the number of bridging water molecules predicted for each complex are given. The results indicate that the non-electrostatic energy change ranges from -15.6 to 1.3 kcal/mol and the electrostatic energy change ranges from -83.1 to -20.4 kcal/mol. These energy variations are much larger than the experimental free energy variations (4.6 kcal/mol). This suggests that the effects other than solute enthalpy should be important in determining the potencies of compounds. The polar and non-polar surface area changes vary from -153.7 to -63.3 Å^2 and -185.8 to -78.9 Å^2, respectively. The negativity indicates the burial of the surface areas upon binding. The number of rotatable bonds (as defined in the Methodology section) of each compound varies from 0 to 12. The number of bridging water molecules varies from 2 to 5.

The six terms presented in Table 3 were fitted to the experimental binding free energies for all the 35 compounds with the standard least-square-fitting

method. The predictive power was then assessed using a leave-one-out cross-validation procedure. It was further assessed using the 'five-group cross-validation' procedure: the compound set is divided into five independent groups of equal sizes and each of the groups is predicted from the rest of the groups. The 'five-group cross-validation' is a robust test in which one fifth of the compounds is predicted from the other independent compounds. The correlation coefficient between the predicted and experimental binding free energies, r^2, q^2 of leave-one-out cross-validation and q^2 of 'five-group cross-validation' are given in the first row of Table 4. The correlation coefficient is high (0.83) and the quality of fit is good ($r^2 = 0.69$). The leave-one-out cross-validation indicates that the free energy model has reasonable predictive ability ($q^2 = 0.51$). The 'five-group cross-validation' indicates that the free energy model derived from 28 compounds can reasonably predict the activities of an 'external' set of 7 compounds ($q^2 = 0.55$).

A comparison of predicted *versus* experimental binding free energies is given in Figure 3. It appears that compound 22 is an outlier. Removing this compound from the list gave a better fit except that the q^2 of 'five-group cross-validation' dropped to -0.15. For improving the model, we examined the derived values of the scaling parameters of the six terms (see the first and second rows in Table 5). The scaling parameter a_5, which is related to the number of rotatable bonds in a compound, exhibits small negative values. The negativity implies that a compound with more rotatable bonds tends to be more favorable for binding. This is opposite to the physical role of this term that accounts for the loss of conformational entropy of a compound upon binding and is expected to be more unfavorable to binding when a compound
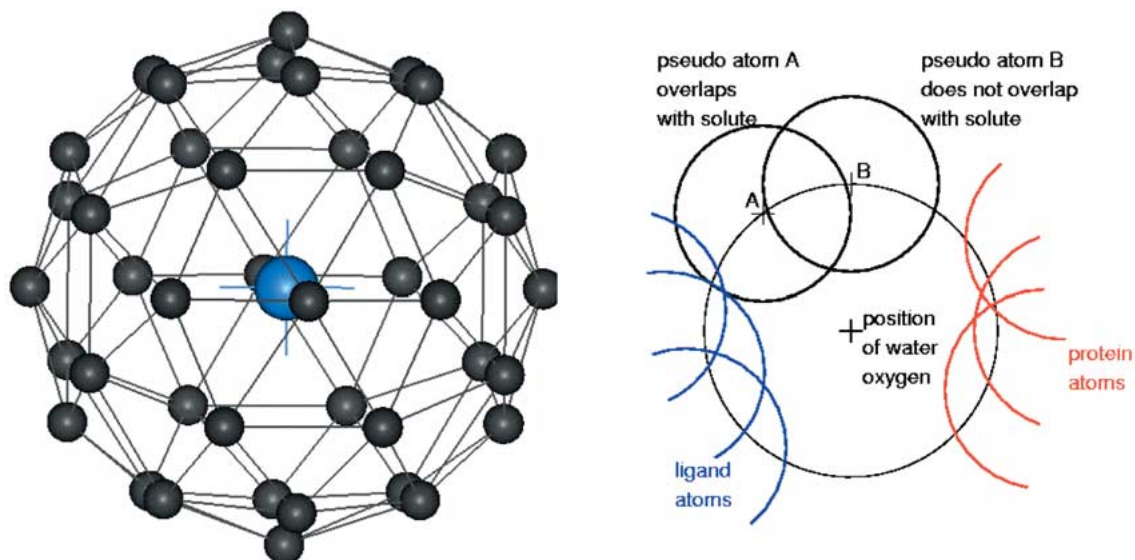
Figure 1. Algorithmic determination of exposure of a water molecule. In the left panel, a regular icosahedron was centered on the water oxygen atom and a pseudo-atom was put at each vertex and the midpoint of each edge of the icosahedron, totaling 42 pseudo-atoms. In the right panel, a pseudo-atom has a radius of 1.5 Å and is 2.5 Å away from the water oxygen. Pseudo-atom B does not overlap with any solute atoms but pseudo-atom A does. If more than two (out of the 42) pseudo-atoms do not overlap with any solute atoms, the water is considered exposed and is deleted.

is more flexible. It is thus justifiable to consider this term as a non-correlative term. We omitted this term and performed another least-square fitting with the full compound set and with the same outlier (compound 22) excluded. The results are given in the third and fourth rows of Tables 4 and 5. The q^2 of 'five-group cross-validation' without the outlier is now increased to 0.69 while the other indexes measuring the quality of fit and predictability are either similar or slightly improved for both the full compound set and the set without the outlier.

We noticed that the scaling parameters of non-polar and polar surface areas were very small. These small terms could be other sources of noise. We further omitted the non-polar surface term and refit the data with and without the outlier. The results are given in the fifth and sixth rows of Tables 4 and 5. Finally, we omitted all the small contribution terms (polar, non-polar and number of rotatable bonds). The results are given in the seventh and eighth rows of Tables 4 and 5. All the indexes in Table 4 that correspond to the minimum number of terms are similar or better than those based on more terms. In particular, the q^2 values (predictability) reach 0.60 and 0.62 for the full compound set and 0.67 and 0.70 if the outlier is excluded. The correlation coefficient and r^2 also reach a good level (0.86 and 0.74).

The scaling parameters of all the terms are remarkably stable upon different conditions of fit (Table 5). Specifically, the scaling parameters of the non-electrostatic and electrostatic terms vary from 0.091 to 0.153 and from 0.064 to 0.079, respectively. The scaling parameter for the number of bridging water molecules varies from 0.64 to 0.76 kcal/mol per water molecule. And the constant term varies from 5.49 to 5.88 kcal/mol. (Note: the constant term would be increased by 8.23 kcal/mol if mole instead of micromole concentration unit was used in Eq. 6.) This degree of stability is another indication of the robustness of the free energy model.

Summarizing the above results, a binding free energy function with minimum number of terms for PTP1B inhibitors can be given as follows,

$$\Delta G = 0.134 \Delta E^{ne} + 0.078 \Delta E^{e} + 0.72n + 5.5. \tag{8}$$

In order to examine the robustness of the model, the same analysis was performed with the dielectric constant set to 2r instead of 4r. The analysis included re-minimization of free and bound states with the new dielectric constant, re-calculation of energy components and surface areas, and fitting to experimental binding free energies with full and partial terms with and without outlier. The best binding free energy
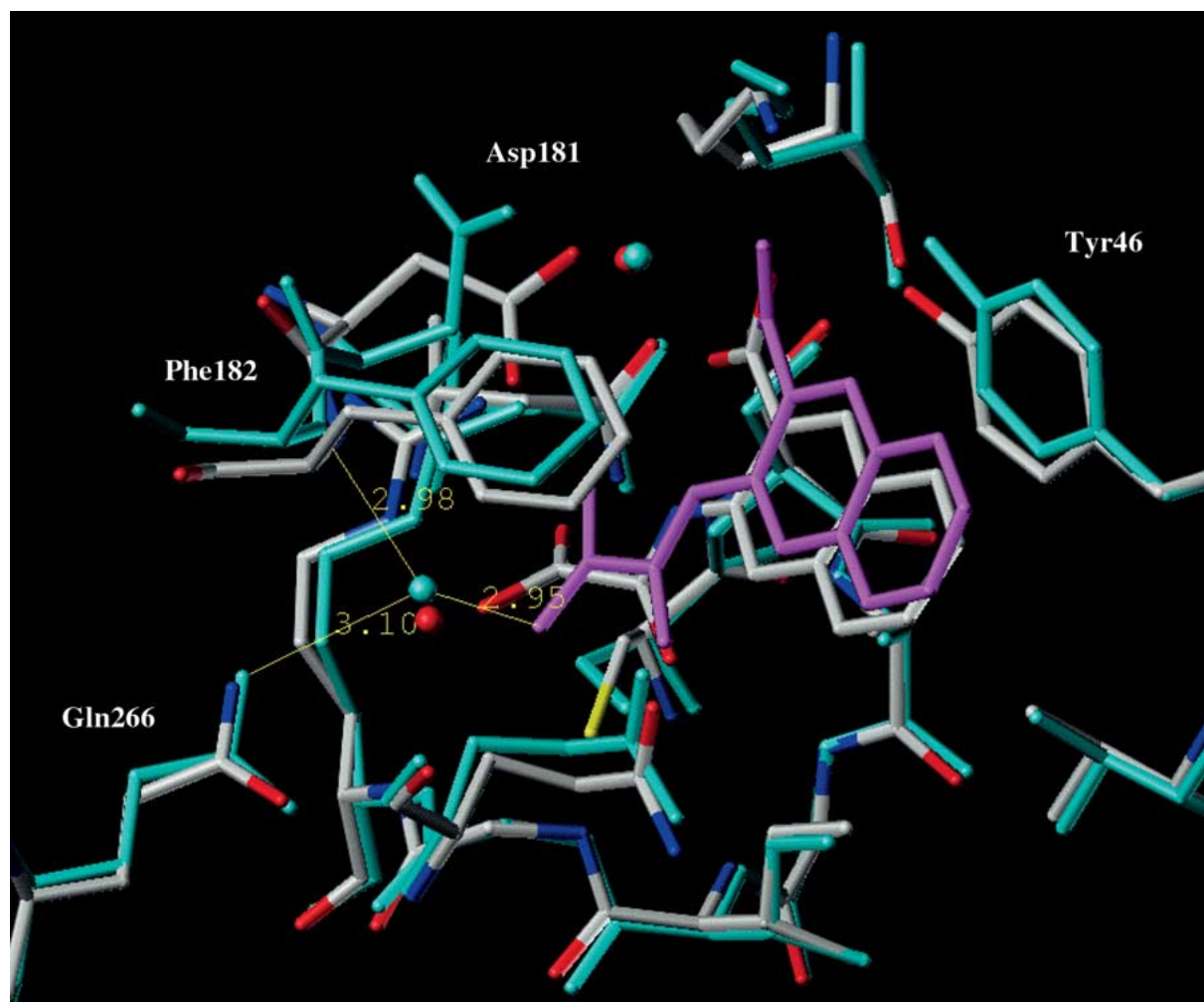
Figure 2. Comparison of predicted bridging water molecules with those of a crystal structure. All atoms in the calculated structure are in light blue. Atom types C, O, and N in the crystal structure are in white, red, and blue, respectively.

model obtained is as follows,

$$\Delta G \ = \ 0.091 \Delta E^{ne} + 0.042 \Delta E^{e} +$$
$$0.0122 \Delta A^{npol} + 0.72n + 6.0. \quad (9)$$

The correlation coefficients, r^2, q^2 of leave-one-out cross-validation and q^2 of 'five-group cross-validation' are, respectively, 0.87, 0.76, 0.66, and 0.68 (with the same outlier, compound 22, excluded). This model bears the same level of correlation and predictive power as the model with dielectric constant of 4r. In comparison to Eq. 8, the scaling parameter of the electrostatic term in Eq. 9 is reduced almost by half, in accordance with the reduction of the dielectric constant. The contribution of non-polar surface area is increased to the important magnitude, indicating that the solvation effect needs to be computed through surface area changes when a small dielectric constant is used (see Discussion for explanation). The scaling parameters for non-electrostatic term and bridging water term and the constant term are relatively unchanged. The contributions of polar surface area and rotatable bonds are still negligible.

Discussion and conclusions

An open conformation and a closed conformation of PTP1B have been found in the co-crystal structures with different inhibitors and substrates [18]. The open conformation is different from the closed one in the disposition of the WPD-loop where Asp181 is moved from the catalytic position to a remote position. The

Table 3. Calculated changes in non-electrostatic energy, electrostatic energy, polar surface area, nonpolar surface area, number of contributing rotatable bonds and number of bridging waters upon binding of each compound*.

Compound ID	ΔE^{ne}	ΔE^e	ΔA^{pol}	ΔA^{npol}	m	n
1	−4.1	−50.9	−86.5	−91.5	1	2
2	−14.2	−27.6	−95.4	−107.0	1	2
3	−6.2	−29.3	−83.3	−100.3	1	2
4	−7.8	−21.0	−105.0	−99.9	1	2
5	−15.6	−20.4	−112.8	−100.9	1	2
6	−10.9	−28.3	−63.3	−91.9	1	2
7	−10.5	−29.3	−64.7	−99.5	1	2
8	−6.1	−39.0	−91.4	−102.8	2	2
9	−7.4	−38.2	−98.5	−98.8	2	2
10	−4.9	−55.4	−102.3	−94.6	1	2
11	−5.7	−60.2	−125.0	−112.4	6	2
12	−4.6	−66.2	−131.0	−131.3	6	2
13	−1.7	−51.3	−82.2	−78.9	0	2
14	−4.3	−51.0	−99.7	−87.6	1	2
15	−3.2	−50.0	−85.8	−90.1	1	2
16	−8.9	−54.3	−74.1	−112.0	1	2
17	−6.6	−56.5	−79.0	−97.3	1	2
18	−2.7	−54.7	−96.7	−93.7	2	2
19	−13.2	−42.0	−99.3	−97.9	0	2
20	−10.1	−41.5	−97.5	−82.6	0	2
21	−13.6	−60.2	−153.2	−185.8	12	2
22	−12.7	−38.4	−95.0	−104.3	0	2
23	−12.0	−41.4	−97.4	−106.3	0	2
24	−12.1	−41.7	−99.2	−112.3	0	2
25	−2.8	−53.7	−88.5	−103.9	1	2
26	−4.3	−52.5	−85.2	−92.0	1	2
27	−5.7	−83.1	−133.6	−133.4	2	5
28	−5.9	−72.7	−82.3	−120.8	1	3
29	0.8	−69.3	−96.1	−96.6	1	2
30	1.3	−68.7	−110.0	−104.4	1	2
31	−7.1	−68.9	−104.4	−104.4	1	2
32	−5.3	−78.2	−153.7	−134.2	2	2
33	−14.7	−83.0	−127.7	−177.5	3	5
34	−7.5	−72.6	−161.3	−158.8	4	2
35	−10.3	−37.4	−78.1	−105.2	2	2

*All energies in kcal/mol and area in Å^2.

seven crystal structures used (Table 1) all have the closed conformation. Our docking was done with the closed conformation for all the compounds. It is possible that compounds 8, 9, and 35, which bear a malonic acid group, might bind to the open conformation or to both the open and closed conformations. A large cyclic compound with a malonic acid group as the phosphate-mimicking moiety was found to bind to the open conformation in the co-crystal structure 1BZH [18]. Our docking of compounds 8, 9, and 35 showed that these small molecules fit well in the closed conformation of PTP1B, although their binding to both the conformations is not excluded.

All the Asp and Glu residues were modeled as anions and Lys and Arg residues as cations. The residues with questionable protonation states in the surroundings of the calculated active site are Asp48 and Asp181. Asp48 was modeled as anion based on

Table 4. Measures of quality of fit and predictive power depending on the inclusion or exclusion of an outlier and sets of terms included in fitting.

Model[a]	Outliers removed	Correlation coefficient	r^2	q^2_{loo} [b]	q^2_{fg} [c]
A		0.83	0.69	0.51	0.55
B	1	0.88	0.77	0.62	−0.15
C		0.83	0.69	0.57	0.58
D	1	0.87	0.76	0.66	0.69
E		0.83	0.69	0.59	0.62
F	1	0.87	0.76	0.67	0.71
G		0.82	0.67	0.60	0.62
H	1	0.86	0.74	0.67	0.70

[a]A: full set, full terms; B: compound 22 excluded, full terms; C: full set, term m excluded; D: compound 22 excluded, term m excluded; E: full set, terms ΔA^{npol} and m excluded; F: compound 22 excluded, terms ΔA^{npol} and m excluded; G: full set, terms ΔA^{pol}, ΔA^{npol} and m excluded; H: compound 22 excluded, terms ΔA^{pol}, ΔA^{npol} and m excluded.
[b]q^2 in leave-one-out cross-validation tests.
[c]q^2 in cross-validation tests by dividing compound set into five groups.

Table 5. Weighting factors relating calculated terms to total binding free energies derived by fitting depending on inclusion or exclusion of an outlier and sets of terms included*.

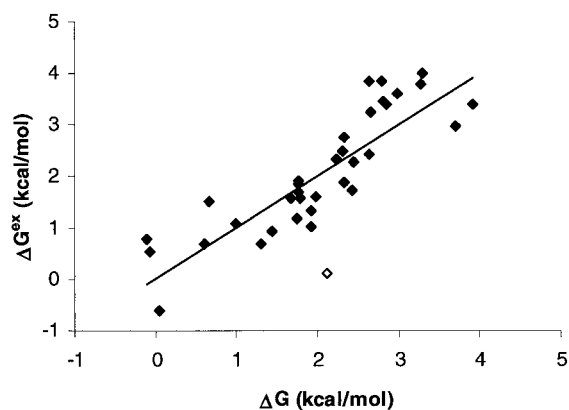| Model	Outliers removed	a_1	a_2	a_3	a_4	a_5	a_6	C
A		0.124	0.067	0.0053	0.0039	−0.005	0.72	5.78
B	1	0.099	0.065	0.0045	0.0034	−0.044	0.64	5.67
C		0.123	0.067	0.0054	0.0044	–	0.72	5.81
D	1	0.091	0.064	0.0050	0.0079	–	0.68	5.88
E		0.134	0.070	0.0074	–	–	0.71	5.78
F	1	0.113	0.069	0.0085	–	–	0.66	5.84
G		0.153	0.079	–	–	–	0.76	5.49
H	1	0.134	0.078	–	–	–	0.72	5.50

*See Eq. 5 for definition of each term.

Figure 3. Comparison of predicted binding free energies ΔG and experimental ones ΔG^{ex} for the full compound set. The trend line is added for visual guidance. The open dot corresponds to an outlier (compound 22).

the fact that this residue serves as double hydrogen bond acceptor in the complexes with substrate-like compounds [13, 18]. It was proposed that Asp181 undergoes a protonation–deprotonation reversible transition in catalytic cycles [51]. Calculation of energetics of this process requires quantum chemistry treatment of the large complex systems, which cannot be done within a reasonable time for the data set of current size. Zhang et al. [52] have demonstrated that mutating Asp181 to Asn or Ala increases the enzyme's affinity to a substrate-like inhibitor from a dissociation constant K_d of 0.24 to 0.12 or 0.04 μM. Therefore, the protonation state of this residue is unlikely to have an important contribution to the binding potencies for ligands. For consistency, we treated this residue the same as the other Asp residues. Cys215 was modeled as thiolate anion [51, 52]. The energy minimizations with such a condition gave rise to a contact distance

of around 3.5 Å between the S$^-$ and the phosphorus atom in the compounds containing difluoromethyl phosphate as phosphate mimetic. The corresponding contact distance is about 3.72 Å in crystal structures [53]. The favorable comparison votes for the credit of the MMFF94 force-field used.

The free energy function used in the fitting process was derived based on a regular decomposition (see the Methodology section). The free energy change of a system upon a process of molecular association and conformational change was expressed as the contribution due to the intra- and intermolecular energy changes of solutes, that of solvation free energy changes, and that of configurational entropy changes [24, 46]. The solute energy contribution was calculated using the force-field energy. The solvation free energy contribution was approximated using the polar and non-polar surface areas. The configurational entropy contribution was approximated using the number of rotatable bonds that are considered 'frozen' upon a binding process. While these quantities were calculated in the modeling, the coefficients relating these quantities to the experimentally observable free energy change are unknown. We determined the coefficients by fitting the calculated quantities with the experimental binding free energies. Such a rigorous treatment was critical to the success of finding reasonable correlation, and even more important for assuring the predictive power of the derived function.

The derived free energy functions (Eqs. 8 and 9) are clearly able to predict the potencies of the inhibitors for association with the active site of PTP1B. This was demonstrated by the leave-one-out cross-validation and 'five-group' cross-validation. In the 'five-group' cross-validation, the free energy functions derived from test sets of 28 compounds were able to predict 'external' sets of seven compounds. Moreover, the scaling parameters were stable in the functions derived with test sets (data not shown) and in the function derived with the full set.

The scaling parameters preceding the non-electrostatic energy and electrostatic energy in Eq. 8 are relatively small. This reflects, in our opinion, the contributions of general solvation effects. The solvation effects on the electrostatic energy can be understood by the known dielectric screening effect of water, which largely reduces the strength of electrostatic interactions between solutes. The non-electrostatic energy, which is primarily comprised of van der Waals interactions, is also largely screened by the solvent medium. It can be understood in that the

formation of atom-atom contacts between solutes (or even within solutes) occurs at the expense of solute-solvent contacts. The van der Waals interaction energy gained between and within solutes is thus opposed and differed by the loss in solute-solvent interactions. The residual of such a balance, which contributes to the final free energy, is thus much smaller than the pure solute-solute energy. Such an effect is effectively reflected as a reducing scaling factor to the non-electrostatic energy. However, the positive sign of the scaling factor suggests that the solute-solute interactions are the driving force for the molecular association.

We originally intended to use the surface areas to account for the general solvation contributions. However, when a dielectric constant of 4r was used, very small scaling parameters for the surface areas were derived in the least-square-fitting experiments. The corresponding terms with such small scaling parameters are unlikely to have accounted for expected solvation effects. Alternatively, the solvation effects could have been transferred into the scaling factors, reducing the solute interaction energies. When we imposed the larger scaling parameters to the surface terms in the least-square-fitting experiments, larger scaling parameters to the solute energies were found (data not shown). It appears that the surface areas were interdependent with the solute energies and could not be de-coupled in the least-square fitting when both the types were used in fitting. (Partial-Least-Square (PLS) [54] fitting did not result in a better model.)

When we changed the dielectric constant from 4r to 2r, a free energy model of similar correlation and predictive power was obtained (see Eq. 9). The contribution of non-polar surface area was increased from the negligible level to an important magnitude. About 12.2 cal/mol was credited to binding for every unit Å^2 surface area buried, consistent with the normal hydrophobic energy scale [24]. It appears that the hydrophobic energy was effectively separated from the solute energy terms when a dielectric constant of 2r was used.

We decided not to solve the Poisson–Boltzmann equation to obtain electrostatic solvation energy. Solving the Poisson–Boltzmann equation will be much more time consuming and may not give better results. Perez et al. [28] have studied 49 HIV-1 protease inhibitors and found that computation of the Poisson–Boltzmann solvation energy did not give a better model than the simple calculation of molecular interaction energy.

Calculation of configurational or conformational entropy is an unsolved difficult problem. It has not been demonstrated so far that this entropy should be generally important for small molecule binding. A number of calculations of ligand binding [27–31] have been performed without invoking this term, and still generated reasonable correlations with experimental binding activities. This suggests that this entropy term may not be important. Consistent with other people's findings, our calculations indicate that inclusion of compound entropy is not necessary for achieving a good correlation. Giving the fact that a free energy function without a conformational entropy term can capture the trend of binding activities, we could not rule out that inclusion of protein conformational entropy might improve the correlation. Due to the complexity of the problem, we leave this question to the future studies of ourselves and other researchers.

A water molecule can help the association of solute molecules by forming bridging hydrogen bonds between them. This stabilization effect has been taken into account in the calculations of ΔE^e and ΔE^{ne}. The term related to the number of bridging water molecules in Eqs. 8 or 9 accounts for the remaining contributions, namely, the free state enthalpies and the free to bound state entropy changes of bridging water molecules. The free state enthalpy of a bridging water molecule would be the same as that of any bulk water molecule, representing attractive interaction energies with the surrounding congener molecules. It thus stabilizes the free state or works against binding. The entropy of a water molecule decreases upon being trapped in a complex in a bridging process, which also works against binding. The positive scaling parameter for this term in Eqs. 8 or 9 is consistent with the expected role. The derived value implies that the engagement of a water molecule in a complex is opposed by 0.72 kcal/mol, in compensation with the strengthened molecular interactions in the complex. The magnitude of the latter depends on the microenvironment of the trapped water.

In summary, we found a free energy function and procedure that is able to predict the binding activities of compounds toward PTP1B based on docking studies. The signs of the component terms clearly indicated that the binding processes are driven by van der Waals type interactions and hydrogen bonding between solutes. These interactions are tightly correlated with the shape matching and electrostatic pairing between ligand and protein. Thus, our finding is consistent with the classical view of molecular re-

cognition. The roles of aqueous solvent are multiple: it largely reduces the magnitudes of the driving forces on one hand, and helps the binding processes through water bridge formation and hydrophobic effect on the other. The gained insights are very useful in designing new inhibitors for this important drug target.

References

1. Burke, Jr., T.R. and Zhang, Z.-Y., Biopolymers, 47 (1998) 225.
2. Møller, N.P.H., Iversen, L.F., Andersen, H.S. and McCormack, J.G., Curr. Opin. Drug Dis. Dev., 3 (2000) 527.
3. Ahmad, F., Li, P.-M., Meyerovitch, J. and Goldstein, B.J., J. Biol. Chem., 270 (1995) 20503.
4. Kenner, K.A., Anyanwu, E., Olefsky, J.M. and Kusari, J., J. Biol. Chem., 271 (1996) 19810.
5. Kole, H.K., Garant, M.J., Kole, S. and Bernier, M., J. Biol. Chem., 271 (1996) 14302.
6. Bandyopadhyay, D., Kusari, A., Kenner, K.A., Liu, F., Chernoff, J., Gustafson, T.A. and Kusari, J., J. Biol. Chem., 272 (1997) 1639.
7. Chen, H., Wertheimer, S.J., Lin, C.H., Amrein, K.E., Burn, P. and Quon, M.J., J. Biol. Chem., 272 (1997) 8026.
8. Kusari, J., Kenner, K.A., Suh, K.-I., Hill, D.E. and Henry, R.R., J. Clin. Invest., 93 (1994) 1156.
9. Ahmad, F., Azevedo, J.L., Cortright, R., Dohm, G.L. and Goldstein, B.J., J. Clin. Invest., 100 (1997) 449.
10. Ahmad, F., Considine, R.V., Bauer, T.L., Ohannesian, J.P., Marco, C.C. and Goldstein, B.J., Metabolism, 46 (1997) 1140.
11. Elchelby, M., Payette, P., Michaliszyn, E., Cromlish, W., Collins, S., Lee Loy, A., Normandin, D., Cheng, A., Himms-Hagen, J., Chan, C.-C., Ramachandran, C., Gresser, M.J., Tremblay, M.L. and Kennedy, B.P., Science, 283 (1999) 1544.
12. Chernoff, J., Schievella, A.R., Jost, C.A., Erikson, R.L. and Neel, B.G., Proc. Natl. Acad. Sci. USA, 87 (1990) 2735.
13. Salmeen, A., Andersen, J.N., Myers, M.P., Tonks, N.K. and Barford, D., Mol. Cell., 6 (2000) 1401.
14. Ahmad, F. and Goldstein, B.J., Biochim. Biophys. Acta, 1248 (1995) 57.
15. Tonks, N.K. and Neel, B.G., Curr. Opin. Cell Biol., 13 (2001) 182.
16. Malamas, M.S., Sredy, J., Gunawan, I., Mihan, B., Sawicki, D.R., Seestaller, L., Sullivan, D. and Flam, B.R., J. Med. Chem., 43 (2000) 995.
17. Sarmiento, M., Puius, Y.A., Vetter, S.W., Keng, Y.-F., Wu, L., Zhao, Y., Lawrence, D.S., Almo, S.C. and Zhang, Z.-Y., Biochemistry, 39 (2000) 8171.
18. Groves, M.R., Yao, Z.J., Roller, P.P., Burke Jr, T.R. and Barford, D., Biochemistry, 37 (1998) 17773.
19. Andersen, H.S., Iversen, L.F., Jeppesen, C.B., Branner, S., Norris, K., Rasmussen, H.B., Moller, K.B. and Moller, N.P., J. Biol. Chem., 275 (2000) 7101.
20. Iversen, L.F., Andersen, H.S., Branner, S., Mortensen, S.B., Peters, G.H., Norris, K., Olsen, O.H., Jeppesen, C.B., Lundt, B.F., Ripka, W., Moller, K.B. and Moller, N.P., J. Biol. Chem., 275 (2000) 10300.
21. Wrobel, J., Sredy, J., Moxham, C., Dietrich, A., Li, Z., Sawicki, D.R., Seestaller, L., Wu, L., Katz, A., Sullivan, D., Tio, C. and Zhang, Z.-Y., J. Med. Chem., 42 (1999) 3199.
22. Martin, Y. C., Quantitative Drug Design: A Critical Introduction, Marcel Dekker Inc., New York, Basel, 1978.

23. Jorgensen, W.L., Acc. Chem. Res., 22 (1989) 184.
24. Wang, J., Szewczuk, Z., Yue, S.-Y., Tsuda, Y., Konishi, Y. and Purisima, E.O., J. Mol. Biol., 253 (1995) 473.
25. Luo, R. and Gilson, M.K., J. Am. Chem. Soc., 122 (2000) 2934.
26. Hou, T., Zhu, L., Chen, L. and Xu, X., J. Chem. Inf. Comput. Sci., 43 (2003), 273.
27. Holloway, M.K., Wai, J.M., Halgren, T.A., Fitzgerald, P.M., Vacca, J.P., Dorsey, B.D., Levin, R.B., Thompson, W.J., Chen, L.J. and deSolms, S.J., J. Med. Chem., 38 (1995) 305.
28. Perez, C., Pastor, M., Ortiz, A.R. and Gago, F., J. Med. Chem., 41 (1998) 836.
29. Kulkarni, S.S. and Kulkarni, V.M., J. Chem. Inf. Comput. Sci., 39 (1999) 1128.
30. Sippl, W., J. Comput.-Aided Mol Des., 14 (2000) 559.
31. Jiang, H., Chen, K., Tang, Y., Chen, J., Li, Q., Wang, Q. and Ji, R., J. Med. Chem., 40 (1997) 3085.
32. Kroemer, R.T., Ettmayer, P. and Hecht, P., J. Med. Chem., 38 (1995) 4917.
33. Sippl, W., Contreras, J.M., Parrot, I., Rival, Y.M. and Wermuth, C.G., J. Comput.-Aided Mol. Des., 15 (2001) 395.
34. Cramer III, R.D., Patterson, D.E. and Bunce, J.D., J. Am. Chem. Soc., 110 (1988) 5959.
35. Sippl, W., Bioorg. Med. Chem., 10 (2002) 3741.
36. Liu, H., Huang, X., Shen, J., Luo, X., Li, M., Xiong, B., Chen, G., Shen, J., Yang, Y., Jiang, H. and Chen, K., J. Med. Chem., 45 (2002) 4816.
37. Cheng, F., Shen, J., Luo, X., Zhu, W., Gu, J., Ji, R., Jiang, H. and Chen, K., Bioorg. Med. Chem., 10 (2002) 2883.
38. Buolamwini, J.K. and Assefa, H., J. Med. Chem., 45 (2002) 841.
39. Constantino, G., Macchiarulo, A., Camaioni, E. and Pellicciari, R., J. Med. Chem., 44 (2001) 3786.
40. Murthy, V.S. and Kulkarni, V.M., Bioorg. Med. Chem., 10 (2002) 897.
41. Burke Jr., T.R., Ye, B., Yan, X., Wang, S., Jia, Z., Chen, L., Zhang, Z.-Y. and Barford, D., Biochemistry, 35 (1996) 15989.
42. Yao, Z.-J., Ye, B., Wu, X.-W., Wang, S., Wu, L., Zhang, Z.-Y. and Burke Jr., T.R., Bioorg. Med. Chem., 6 (1998) 1799.
43. Kotoris, C.C., Chen, M.-J. and Taylor, S.D., Bioorg. Med. Chem. Lett., 8 (1998) 3275.
44. Taylor, S.D., Kotoris, C.C., Dinaut, A.N., Wang, Q., Ramachandran, C. and Huang, Z., Bioorg. Med. Chem., 6 (1998) 1457.
45. Wang, Q., Huang, Z., Ramachandran, C., Dinaut, A.N. and Taylor, S.D., Bioorg. Med. Chem. Lett., 8 (1998) 345.
46. Wang, J. and Purisima, E.O., J. Am. Chem. Soc., 118 (1996) 995.
47. SYBYL 6.6 molecular modeling software; Tripos Associates Inc., St. Louis, MO, 2000.
48. Halgren, T.A., J. Comput. Chem., 17 (1996) 490.
49. Powell, M.J.D., Mathematical Programming, 12 (1997) 241.
50. Insight II, Release 98.0, 1998, Molecular Simulations Inc., San Diego, CA, 1998.
51. Denu, J.M., Lohse, D.L., Vijayalakshmi, J., Saper, M.A. and Dixon, J.E., Proc. Natl. Acad. Sci. USA, 93 (1996) 2493.
52. Zhang, Y.-L., Yao, Z.-J., Sarmiento, M., Wu, L., Burke, Jr. T.R. and Zhang, Z.-Y., J. Biol. Chem., 275 (2000) 34205.
53. Asante-Appiah, E., Patel, S., Dufresne, C., Roy, P., Wang, Q., Patel, V., Friesen, R.W., Ramachandran, C., Becker, J.W., Leblanc, Y., Kennedy, B.P. and Scapin, G., Biochemistry, 41 (2002) 9043.
54. Wold, S., In Kubinyi, H. (Ed.), 3D-QSAR in Drug Design: Theory, Methods and Applications, 1993, ESCOM Science Publishers, Leiden, The Netherlands.